Optimal Base Station Antenna Downtilt in Downlink Cellular Networks

Junnan Yang, Student Member, IEEE, Ming Ding, Senior Member, IEEE,
Guoqiang Mao, Fellow, IEEE, Zihuai Lin, Senior Member, IEEE, De-gan
Zhang, Member, IEEE, Tom Hao Luan, Member, IEEE

Abstract

From very recent studies, the area spectral efficiency (ASE) performance of downlink (DL) cellular networks will continuously decrease and finally to zero with the network densification in a fully loaded ultra-dense network (UDN) when the absolute height difference between a base station (BS) antenna and a user equipment (UE) antenna is larger than zero, which is referred as the ASE Crash. We revisit this issue by considering the impact of the BS antenna downtilt on the downlink network capacity. In general, there exists a height difference between a BS and a UE in practical networks. It is common to utilize antenna downtilt to adjust the direction of the vertical antenna pattern, and thus increase received signal power or reduce inter-cell interference power to improve network performance. This paper focuses on investigating the relationship between the base station antenna downtilt and the downlink network capacity in terms of the coverage probability and the ASE. The analytical results of the coverage probability and the ASE are derived, and we find that there exists an optimal antenna downtilt to achieve the maximal coverage probability for each base station density. Moreover, we derive numerically solvable expressions for the optimal antenna downtilt, which is a function of the base station density. Our theoretical and numerical results show that after applying the optimal antenna downtilt, the network performance can be improved significantly. Specifically, with the optimal antenna downtilt, the ASE crash can be delayed by nearly one order of magnitude in terms of the base station density.

Index Terms

Antenna downtilt, Ultra-dense networks (UDNs), Coverage probability, Area spectral efficiency (ASE), Stochastic geometry.

I. INTRODUCTION

It has been widely acknowledged that wireless networks continue to face significant challenges and opportunities. From 1950 to 2000, the wireless network capacity has increased around 1 million fold [1]. In the first decade of 2000, network densification continued to fuel the 3rd Generation Partnership Project (3GPP) 4th-generation (4G) Long Term Evolution (LTE) networks, and is expected to remain as one of the main forces to drive the 5th-generation (5G) networks onward [2]. Various emerging technologies have been used in cellular networks, such as small cell networks (SCNs), ultra-dense networks (UDNs), cognitive radio, massive MIMO, etc [3]. In particular, in the past few years, a few noteworthy studies have been carried out to revisit the performance analyses for cellular networks under more practical propagation assumptions. In [4], the authors considered a multi-slope piece-wise path loss function, while in [5], the authors investigated line-of-sight (LoS) and non-line-of-sight (NLoS) transmission as a probabilistic event for a millimeter wave communication scenario. The most important finding in these two works is that the per-BS coverage probability performance starts to decrease when the base station (BS) density is sufficiently large. Fortunately, such decrease of the coverage probability will not change the monotonic increase of the area spectral efficiency (ASE) as the BS density increases [4, 5]. However, in very recent works, the authors found that the ASE performance will continuously decrease toward zero with the network densification for UDNs when the absolute height difference between a base station antenna and a user equipment (UE) antenna is larger than zero, which is referred as the ASE Crash in [6–8].

Having a closer look at the problem, we realize that in a three-dimensional (3D) channel model, the antenna pattern and downtilt may bring a gain to received signal and at the same time reduce inter-cell interference [9]. The benefits of horizontal beamforming in cellular networks are well-understood and such technology has already been adopted in the LTE networks. However, vertical beamforming (based on an antenna downtilt) receives much less attention. Recent studies have made some initial efforts in shedding new light on the impact of antenna downtilt on the cellular network [10–12], but most of these studies were solely based on computer simulations.

In this paper, we investigate the impact of the antenna pattern and downtilt on the per-

formance of the downlink (DL) cellular networks, in terms of the coverage probability and the area spectral efficiency. We also derive the analytical expressions for the optimal antenna downtilt that resulting in the best coverage probability of the network given a certain BS density.

Compared with the existing works, the main contributions of this paper are:

- We analytically investigate the relationship between the the antenna downtilt and the cellular network performance in terms of the coverage probability and the ASE. From our theoretical results, we find that there is a tradeoff between increasing the received signal and reducing the interference, and hence there exists an optimal antenna downtilt to achieve the maximal coverage probability for each BS density.

- We derive numerically solvable expressions for the optimal antenna downtilt with a certain BS density. In particular, there are three components, namely the LoS part, the NLoS part and the noise part, leading to the optimal antenna downtilt. Moreover, we provide analytical results of the coverage probability and the ASE assuming the optimal antenna downtilt.

- Our theoretical and numerical results demonstrate that the performance of the cellular network can be improved significantly using the optimal antenna downtilt. In particular, applying the optimal antenna downtilt can delay the ASE crash by nearly one order of magnitude in terms of the base station density. Using the derived expressions and the simulation results, network operators can determine the antenna downtilt of BSs to achieve the optimal system throughput.

The rest of this paper is structured as follows. Section II provides a brief review on the related work. Section III describes the system model of the 3D cellular network. Section IV presents our theoretical results on the coverage probability, the optimal antenna downtilt and the network's performance with the optimal antenna downtilt. The numerical results are discussed in Section V, with remarks shedding new light on the network deployment. Finally, the conclusions are drawn in Section VI.

II. RELATED WORK

Stochastic geometry, which is accurate in modeling irregular deployment of base stations (BSs) and mobile user equipment (UEs), has been widely used to analyze the network per-

formance [13, 14]. Andrews, et al. conducted network performance analyses for the downlink (DL) [13] and the uplink (UL) [14] of SCNs, in which UEs and/or BSs were assumed to be randomly deployed according to a homogeneous Poisson point process (HPPP). Furthermore, a stochastic model of the 3D environment was used to evaluate the network performance [6, 15]. In [6], Ming, et al. presented a new finding that if the absolute height difference between BS antenna and UE antenna is larger than zero, then the ASE performance will continuously decrease toward zero with the network densification for UDNs.

Many researchers have realized that a practical antenna can target its antenna beam towards a given direction via downtilt in the vertical domain, which may effect the network performance [9, 16, 17]. For example, the authors in [9] found that the antenna downtilt could bring a significant improvement to the cellular network capacity via computer simulations. In [16], the authors showed that the vertical beamforming could increase SIR by about 5-10 dB for a set of UE locations. N. Seifi and M. Coldrey investigated the performance impact of using antenna downtilt in traditional hexagonal 3D cellular networks in [17]. As we can see, most of the works that investigated the effect of the antenna downtilt using field trials or simulations. To the best of our knowledge, none of the existing works have theoretically analyzed the impact of the antenna downtilt of BSs on the cellular network performance .

In this work, we will investigate the impact of the antenna pattern and downtilt on the performance of the downlink (DL) cellular networks and derive the analytical expressions for the optimal antenna downtilt to achieve the best coverage probability of the network for each certain BS density.

III. System Model

In this section, we will first explain the scenario of the 3D random cellular network. Then, we will present the antenna patterns and user association scheme used in this work.

A. Scenario Description

We consider a 3D random cellular network with downlink (DL) transmissions, where BSs are deployed on a plane according to an HPPP Φ of intensity λ_B BSs/km^2. UEs are also Poissonly distributed in the considered area with an intensity of λ^{UE} UEs/km^2. Note that λ^{UE} is assumed to be sufficiently larger than λ_B so that each BS has at least one associated UE in

its coverage [13, 18, 19]. The two-dimensional (2D) distance between an arbitrary BS and an arbitrary UE is denoted by r in m. Moreover, the absolute antenna height difference between a BS and a UE is denoted by L. Note that the value of L is in the order of several meters. Hence, the 3D distance w between a BS and a UE can be expressed as

$$w = \sqrt{r^2 + L^2}, \tag{1}$$

where $L = H - h$, H is the antenna height of BS and h is the antenna height of UE. Intuitively, the antenna height of BS should decrease as the network becomes dense, however, there is no consensus on the formula about how H should decrease with an increase in λ_B. In this paper, we assume that H, and thus L, are constants. For the current 4G networks, L is around $8.5m$ because the BS antenna height and the UE antenna height are assumed to be $10m$ and $1.5m$, respectively [10].

In addition, we incorporate both NLoS and LoS transmissions into the path loss model. Following [7, 19], we adopt a very general path loss model, in which the path loss $\zeta(w)$, as a function of the distance r, is segmented into N pieces written as

$$\zeta(w) = \begin{cases} \zeta_1(w), & \text{when } 0 \leq w \leq d_1 \\ \zeta_2(w), & \text{when } d_1 < w \leq d_2 \\ \vdots & \vdots \\ \zeta_N(w), & \text{when } w > d_{N-1} \end{cases}, \tag{2}$$

where each piece $\zeta_n(w), n \in \{1, 2, \ldots, N\}$ is modeled as

$$\zeta_n(w) = \begin{cases} \zeta_n^{\mathrm{L}}(w) = A^{\mathrm{L}} w^{-\alpha_n^{\mathrm{L}}}, & \text{LoS Probability: } \mathrm{Pr}_n^{\mathrm{L}}(w) \\ \zeta_n^{\mathrm{NL}}(w) = A^{\mathrm{NL}} w^{-\alpha_n^{\mathrm{NL}}}, & \text{NLoS Probability: } 1 - \mathrm{Pr}_n^{\mathrm{L}}(w) \end{cases}, \tag{3}$$

where

- $\zeta_n^{\mathrm{L}}(w)$ and $\zeta_n^{\mathrm{NL}}(w), n \in \{1, 2, \ldots, N\}$ are the n-th piece path loss functions for the LoS transmission and the NLoS transmission, respectively,

- A^{L} and A^{NL} are the path losses at a reference distance $w = 1$ for the LoS and the NLoS cases, respectively,

- α_n^{L} and α_n^{NL} are the path loss exponents for the LoS and the NLoS cases, respectively.
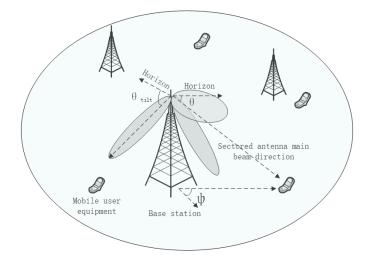
Figure 1. An illustration of the 3D network with randomly deployed base stations and mobile users

In practice, A^{L}, A^{NL}, α_n^{L} and α_n^{NL} are constants obtainable from field tests and continuity constraints [20].

As a special case, we consider a path loss function adopted in the 3GPP [21] as

$$\zeta\left(w\right) = \begin{cases} A^{\mathrm{L}}w^{-\alpha^{\mathrm{L}}}, & \text{LoS Probability: } \mathrm{Pr}^{\mathrm{L}}\left(w\right) \\ A^{\mathrm{NL}}w^{-\alpha^{\mathrm{NL}}}, & \text{NLoS Probability: } 1 - \mathrm{Pr}^{\mathrm{L}}\left(w\right) \end{cases}, \tag{4}$$

together with a linear LoS probability function as follows [21],

$$\mathrm{Pr}^{\mathrm{L}}\left(r\right) = \begin{cases} 1 - \frac{w}{d_1} & 0 < w \leq d_1 \\ 0 & w > d_1 \end{cases}, \tag{5}$$

where d_1 is the 3D cut-off distance of the LoS link for BS-to-UE links. The adopted linear LoS probability function is very useful because it can include other LoS probability functions as its special cases [7].

Fig.1 shows an example of the resulted network. In this model, BSs transmit at power P_B, a mobile can reliably communicate with a BS only when its downlink signal-to-interference-plus-noise ratio (SINR) with respect to that BS is greater than γ. In addition, each BS has a 3D directional antenna pattern and we denote the vertical antenna downtilt and the angle from the BS to the UE by θ_{tilt} and θ, respectively.

B. 3D Antenna Patterns

3D antenna patterns are introduced in this subsection. According to [10] and [22], the 3D antenna gain $G(\varphi, \theta, \theta_{tilt})$ can be approximated in dBi as

$$G(\varphi, \theta, \theta_{tilt}) = G_h(\varphi) + G_v(\theta, \theta_{tilt}) + G_m, \tag{6}$$

where $G_h(\varphi)$ and $G_v(\theta, \theta_{tilt})$ are the normalized horizontal and vertical antenna gain in dBi, respectively. We consider the horizontal omni antenna in this paper, i.e., $G_h(\varphi) = 0$ dBi. G_m is the maximum antenna gain and we can get $G_m = 8.15dB$ from [21]. For the vertical pattern, we consider the dipole antennas. With electrical downtilt [22], the vertical pattern of the dipole antenna main lobe can be approximated as

$$G_v(\theta, \theta_{tilt})_{dB} = \max \left\{ 10 \log_{10} |\cos^n (\theta - \theta_{tilt})| , \ F_{v2} \right\}, \tag{7}$$

where $F_{v2} = -12dB$ is the vertical side-lobe level. $n = 47.64$ for a 4-element half-wave dipole antenna and $\theta = \arctan \left(\frac{L}{r} \right)$ is the angle from the BS to the UE, where L is the height difference between the BS to the UE, r is the distance from the transmitter to the receiver. θ_{tilt} is the vertical antenna downtilt.

C. User Association and Performance Metrics

In this paper, we assume a practical user association strategy (UAS), that each UE is connected to the BS with the strongest received power strength [5, 7]. Note that in our previous work [19] and some other existing works, e.g., [4, 13], it was assumed that each UE should be associated with its closest BS. Such assumption is not appropriate for the considered path loss model in Eq.(2), because in practice a UE should connect to a BS offering the largest received signal strength. Such BS does not necessarily have to be the nearest one to the UE, and it could be a farther one with a stronger LoS path.

Based on the above definitions, we define the coverage probability as a probability that a receiver's signal-to-interference-plus-noise ratio (SINR) is above a per-designated threshold γ:

$$p^{\text{cov}} (\lambda_B, \gamma) = \Pr[\text{SINR} > \gamma], \tag{8}$$

where the SINR is calculated as

$$\text{SINR} = \frac{P_B G(\varphi, \theta, \theta_{tilt})\zeta(r)\,g}{I + N_0},\tag{9}$$

where g is the channel gain of Rayleigh fading, which is modeled as an exponential random variable (RV) with the mean of one, and P_B and N_0 are the transmission power of BS and the additive white Gaussian noise (AWGN) power at each UE, respectively. I is the cumulative interference given by

$$I = \sum_{i:\,c_i \in \Phi\setminus signal} P_B G_i(\varphi, \theta_i, \theta_{tilt})\zeta_i(r)\,g_i.\tag{10}$$

Furthermore, similar to [7, 19], the area spectral efficiency in bps/Hz/km^2 can be formulated as

$$A^{\text{ASE}}(\lambda_B, \gamma_0) = \lambda \int_{\gamma_0}^{\infty} \log_2(1+x)\,f_X(\lambda_B, \gamma_0)\,dx,\tag{11}$$

where γ_0 is the minimum working SINR for the considered network, and $f_X(\lambda_B, \gamma_0)$ is the probability density function (PDF) of the SINR observed at the typical receiver for a particular value of λ.

IV. MAIN RESULTS

Using the 3D channel model based on the stochastic geometry theory, we study the performance of the cellular network and derive the optimal antenna downtilt for each certain base station density in this section. Without any loss of generality we assume that the mobile user under consideration is located at the origin.

A. The Coverage Probability

Based on the path loss model in Eq.(4) and the adopted UAS, our results of $p^{\text{cov}}(\lambda_B, \gamma)$ can be summarized as Theorem 1, Lemma 2 and Lemma 3.

Theorem 1. *Considering the path loss model in Eq.(4) and the presented UAS, the probability of coverage $p^{\text{cov}}(\lambda_B, \gamma)$ can be derived as*

$$p^{\text{cov}}(\lambda_B, \gamma) = \int_0^{d_1} \Pr\left[\frac{\text{S}^{\text{L}}}{I_L + I_N + N_0} > \gamma \,\middle|\, r\right] f_{R,1}^{\text{L}}(r)\, dr$$
$$+ \int_0^{d_1} \Pr\left[\frac{\text{S}^{\text{NL}}}{I_L + I_N + N_0} > \gamma \,\middle|\, r\right] f_{R,1}^{\text{NL}}(r)\, dr$$
$$+ \int_{d_1}^{\infty} \Pr\left[\frac{\text{S}^{\text{NL}}}{I_L + I_N + N_0} > \gamma \,\middle|\, r\right] f_{R,2}^{\text{NL}}(r)\, dr \tag{12}$$

where $f_{R,1}^{\text{L}}(r)$, $f_{R,1}^{\text{NL}}(r)$ and $f_{R,2}^{\text{NL}}(r)$ are represented by

$$f_{R,1}^{\text{L}}(r) = \exp\left(-\int_0^{r_1}\left(1 - \Pr^{\text{L}}(u)\right) 2\pi u \lambda_B du\right) \exp\left(-\int_0^r \Pr^{\text{L}}(u)\, 2\pi u \lambda_B du\right)$$
$$\Pr_1^{\text{L}}(r)\, 2\pi r \lambda_B \tag{13}$$

and

$$f_{R,1}^{\text{NL}}(r) = \exp\left(-\int_0^{r_2} \Pr^{\text{L}}(u)\, 2\pi u \lambda_B du\right) \exp\left(-\int_0^r\left(1 - \Pr^{\text{L}}(u)\right) 2\pi u \lambda_B du\right)$$
$$\times \left(1 - \Pr_1^{\text{L}}(r)\right) 2\pi r \lambda_B \tag{14}$$

and

$$f_{R,2}^{\text{NL}}(r) = \exp\left(-\int_0^{r_2} \Pr^{\text{L}}(u)\, 2\pi u \lambda_B du\right) \exp\left(-\int_0^r\left(1 - \Pr^{\text{L}}(u)\right) 2\pi u \lambda_B du\right) 2\pi r \lambda_B, \tag{15}$$

where r_1 and r_2 are given implicitly by the following equations as

$$r_1^2 = \left(\frac{A_L}{A_{NL}}\right)^{-\frac{2}{\alpha_{NL}}} \left(r^2 + L^2\right)^{\frac{\alpha_L}{\alpha_{NL}}} - L^2, \tag{16}$$

and

$$r_2^2 = \left(\frac{A_{NL}}{A_L}\right)^{-\frac{2}{\alpha_L}} \left(r^2 + L^2\right)^{\frac{\alpha_{NL}}{\alpha_L}} - L^2. \tag{17}$$

Proof: See Appendix A. ∎

Besides, to compute $\Pr\left[\frac{\text{S}^{\text{L}}}{I_L + I_N + N_0} > \gamma\right]$ and $\Pr\left[\frac{\text{S}^{\text{NL}}}{I_L + I_N + N_0} > \gamma\right]$ in Theorem 1, we propose Lemma 2 and Lemma 3, respectively.

Lemma 2. $\Pr\left[\frac{S^{L}}{I_L+I_N+N_0} > \gamma\right]$ can be calculated by

$$\Pr\left[\frac{S^{L}}{I_L + I_N + N_0} > \gamma\right] = \exp\left(-\frac{\gamma N_0}{P_B G(\varphi,\theta_r,\theta_{tilt})A^{L}\sqrt{r^2+L^2}^{-\alpha^{L}}}\right)\mathscr{L}_{I_{\mathrm{agg}}}(s)$$

$$= \exp\left(-\frac{\gamma N_0}{P_B G(\varphi,\theta_r,\theta_{tilt})A^{L}\sqrt{r^2+L^2}^{-\alpha^{L}}}\right)$$

$$\times \exp\left(-2\pi\lambda_B \int_{r}^{d_1}(1-\frac{\sqrt{u^2+L^2}}{d_1})\frac{u}{1+\frac{G(\varphi,\theta_r,\theta_{tilt})\sqrt{u^2+L^2}^{\alpha^L}}{\gamma G(\varphi,\theta_u,\theta_{tilt})\sqrt{r^2+L^2}^{\alpha^L}}}du\right)$$

$$\times \exp\left(-2\pi\lambda_B \int_{r_1}^{d_1}(\frac{\sqrt{u^2+L^2}}{d_1})\frac{u}{1+\frac{G(\varphi,\theta_r,\theta_{tilt})A^L\sqrt{u^2+L^2}^{\alpha^{NL}}}{\gamma A^{NL}G(\varphi,\theta_u,\theta_{tilt})\sqrt{r^2+L^2}^{\alpha^L}}}du\right)$$

$$\times \exp\left(-2\pi\lambda_B \int_{d_1}^{\infty}\frac{u}{1+\frac{G(\varphi,\theta_r,\theta_{tilt})A^L\sqrt{u^2+L^2}^{\alpha^{NL}}}{G(\varphi,\theta_u,\theta_{tilt})A^{NL}\gamma\sqrt{r^2+L^2}^{\alpha^L}}}du\right). \tag{18}$$

Proof: See Appendix A. ■

Lemma 3. $\Pr\left[\frac{S^{NL}}{I_L+I_N+N_0} > \gamma\right]$ can be calculated by

$$\Pr\left[\frac{S^{NL}}{I_L + I_N + N_0} > \gamma\right] = \exp\left(-\frac{\gamma N_0}{P_B G(\varphi,\theta_r,\theta_{tilt})A^{NL}\sqrt{r^2+L^2}^{-\alpha^{NL}}}\right)\mathscr{L}_{I_{\mathrm{agg}}}(s),$$

$$= \exp\left(-\frac{\gamma N_0}{P_B G(\varphi,\theta_r,\theta_{tilt})A^{NL}\sqrt{r^2+L^2}^{-\alpha^{NL}}}\right)$$

$$\times \exp\left(-2\pi\lambda_B \int_{r_2}^{d_1}(1-\frac{\sqrt{u^2+L^2}}{d_1})\frac{u}{1+\frac{G(\varphi,\theta_r,\theta_{tilt})A^{NL}\sqrt{u^2+L^2}^{\alpha^L}}{\gamma A^L G(\varphi,\theta_u,\theta_{tilt})\sqrt{r^2+L^2}^{\alpha^{NL}}}}du\right)$$

$$\times \exp\left(-2\pi\lambda_B \int_{r}^{d_1}(\frac{\sqrt{u^2+L^2}}{d_1})\frac{u}{1+\frac{G(\varphi,\theta_r,\theta_{tilt})\sqrt{u^2+L^2}^{\alpha^{NL}}}{\gamma G(\varphi,\theta_u,\theta_{tilt})\sqrt{r^2+L^2}^{\alpha^{NL}}}}du\right)$$

$$\times \exp\left(-2\pi\lambda_B \int_{d_1}^{\infty}\frac{u}{1+\frac{G(\varphi,\theta_r,\theta_{tilt})\sqrt{u^2+L^2}^{\alpha^{NL}}}{\gamma G(\varphi,\theta_u,\theta_{tilt})\sqrt{r^2+L^2}^{\alpha^{NL}}}}du\right) \tag{19}$$

where $\theta_r = \arctan\left(\frac{L}{r}\right)$ *and* $\theta_u = \arctan\left(\frac{L}{u}\right)$.

Proof: See Appendix A. ■

In Theorem 1, $\mathscr{L}_{I_{\mathrm{agg}}}(s)$ is the Laplace transform of I_{agg} evaluated at s including the

LoS interference transmission and that for NLoS transmission. Regarding the computational process to obtain $p^{\text{cov}}(\lambda_B, \gamma)$, three folds of integrals are respectively required. The string variable Path takes the value of 'L' and 'NL' for the LoS case and the NLoS case, respectively.

B. The impact of antenna downtilt on the received signal and the interference

The antenna pattern and downtilt may bring a gain to the received signal power and at the same time reduce inter-cell interference. In this subsection, we will analytically investigate the impact of antenna downtilt on the received signal strength and the interference of the typical UE, respectively.

Lemma 4. *The ratio of the received signal strength of the typical UE with antenna downtilt to that without can be written as*

$$\frac{S_{withG}}{S_{withoutG}} = G(\varphi, \theta_r, \theta_{tilt})$$
$$\overset{(a)}{=} \cos^n\left(\arctan\left(\frac{L}{r}\right) - \theta_{tilt}\right) + 10^{0.815} \tag{20}$$

where L is the antenna height difference between a BS and a UE, $n = 47.64$ for a 4-element half-wave dipole antenna, r is the average distance from the transmitter to the receiver in the network. (a) can be obtained from Eq.(6) when the angel difference $(\theta - \theta_{tilt})$ is small.

Proof: From Theorem 1, the received signal strength with optimal antenna downtilt can be written as

$$S_{withG} = P_B G(\varphi, \theta_r, \theta_{tilt}) \zeta(w) g \tag{21}$$

and the received signal strength without optimal antenna downtilt can be written as

$$S_{withoutG} = P_B \zeta(w) g \tag{22}$$

Plugging these two into Eq.(20), we have Lemma 4, which concludes our proof. ∎

Lemma 4 characterizes the impact of the antenna downtilt on the received signal. Taking $\lambda_B = 10^3$ BSs/km² as an example, when $r = 15.8m$ and $\theta_{optimal} = 36°$, the ratio of the received signal strength with antenna downtilt to that without is 6.2529.

In the following we will investigate the performance gain achieved by bringing down the inter-cell interference power. In Lemma 5, we derive the coverage probability without the

antenna downtilt in interference.

Lemma 5. *The coverage probability that when the interference without the antenna downtilt can be written as*

$$
\begin{aligned}
p_{withouG}^{\text{cov}}\left(\lambda_B, \gamma\right) = &\int_0^{d_1} \exp\left(-2\pi\lambda_B \int_r^{d_1} (1 - \frac{\sqrt{u^2+L^2}}{d_1}) \frac{u}{1 + \frac{G(\varphi,\theta_r,\theta_{tilt})\sqrt{u^2+L^2}^{\alpha^L}}{\gamma\sqrt{r^2+L^2}^{\alpha^L}}} du \right. \\
&-2\pi\lambda_B \int_{r_1}^{d_1} (\frac{\sqrt{u^2+L^2}}{d_1}) \frac{u}{1 + \frac{G(\varphi,\theta_r,\theta_{tilt})A^L\sqrt{u^2+L^2}^{\alpha^{NL}}}{\gamma A^{NL}\sqrt{r^2+L^2}^{\alpha^L}}} du \\
&\left. -2\pi\lambda_B \int_{d_1}^{\infty} \frac{u}{1 + \frac{G(\varphi,\theta_r,\theta_{tilt})A^L\sqrt{u^2+L^2}^{\alpha^{NL}}}{A^{NL}\gamma\sqrt{r^2+L^2}^{\alpha^L}}} du \right) f_{R,1}^{\text{L}}\left(r\right) dr \\
&+\int_0^{d_1} \exp\left(-2\pi\lambda_B \int_{r_2}^{d_1} (1 - \frac{\sqrt{u^2+L^2}}{d_1}) \frac{u}{1 + \frac{G(\varphi,\theta_r,\theta_{tilt})A^{NL}\sqrt{u^2+L^2}^{\alpha^L}}{\gamma A^L\sqrt{r^2+L^2}^{\alpha^{NL}}}} du \right. \\
&-2\pi\lambda_B \int_r^{d_1} (\frac{\sqrt{u^2+L^2}}{d_1}) \frac{u}{1 + \frac{G(\varphi,\theta_r,\theta_{tilt})\sqrt{u^2+L^2}^{\alpha^{NL}}}{\gamma\sqrt{r^2+L^2}^{\alpha^{NL}}}} du \\
&\left. -2\pi\lambda_B \int_{d_1}^{\infty} \frac{u}{1 + \frac{G(\varphi,\theta_r,\theta_{tilt})\sqrt{u^2+L^2}^{\alpha^{NL}}}{\gamma\sqrt{r^2+L^2}^{\alpha^{NL}}}} du \right) f_{R,1}^{\text{NL}}\left(r\right) dr \\
&+\int_{d_1}^{\infty} \exp\left(-2\pi\lambda_B \int_{r_2}^{d_1} (1 - \frac{\sqrt{u^2+L^2}}{d_1}) \frac{u}{1 + \frac{G(\varphi,\theta_r,\theta_{tilt})A^{NL}\sqrt{u^2+L^2}^{\alpha^L}}{\gamma A^L\sqrt{r^2+L^2}^{\alpha^{NL}}}} du \right. \\
&-2\pi\lambda_B \int_r^{d_1} (\frac{\sqrt{u^2+L^2}}{d_1}) \frac{u}{1 + \frac{G(\varphi,\theta_r,\theta_{tilt})\sqrt{u^2+L^2}^{\alpha^{NL}}}{\gamma\sqrt{r^2+L^2}^{\alpha^{NL}}}} du \\
&\left. -2\pi\lambda_B \int_{d_1}^{\infty} \frac{u}{1 + \frac{G(\varphi,\theta_r,\theta_{tilt})\sqrt{u^2+L^2}^{\alpha^{NL}}}{\gamma\sqrt{r^2+L^2}^{\alpha^{NL}}}} du \right) f_{R,2}^{\text{NL}}\left(r\right) dr
\end{aligned}
\tag{23}
$$

where $f_{R,1}^{\text{L}}\left(r\right)$, $f_{R,1}^{\text{NL}}\left(r\right)$ and $f_{R,2}^{\text{NL}}\left(r\right)$ can be found in Theorem 1.

Proof: Note that we consider the antenna downtilt in the received signal of the typical UE and no antenna downtilt in the interference, therefore we have

$$
S_{signal} = P_B G(\varphi, \theta_r, \theta_{tilt})\zeta\left(w\right) g
\tag{24}
$$

and

$$I = \sum_{i:\, c_i \in \Phi_c \backslash signal} P_B \zeta_i\left(r\right) g_i. \tag{25}$$

Plugging these into Theorem 1, we can get Lemma 5, which concludes our proof. ∎

The difference between Theorem 1 and Lemma 5 lies in the antenna downtilt gain on interference. Lemma 5 and Theorem 1 state that when λ_B is small, in order to get the best performance, the chosen antenna downtilt θ_{tilt} approaches zero, as $\theta_u = \arctan\left(\frac{L}{u}\right)$ is also nearly zero. Therefore, the average antenna gain of the aggregation interference is larger than 1, e.g., $\mathbb{E}_u\left[G(\varphi, \theta_u, \theta_{tilt})\right] \approx G_m > 1$, which showing that the results of Lemma 5 is larger than this of Theorem 1. This means that the antenna downtilt increases both the received signal power and the interference power while the former one over-weighs the latter one. On the other hand, when λ_B is extremely large, e.g., in UDNs, $\mathbb{E}_u\left[G(\varphi, \theta_u, \theta_{tilt})\right] \approx F_{v2} + G_m < 1$, hence the result given by Theorem 1 is larger than that in Lemma 5, which means that the antenna downtilt also reduces inter-cell interference. More numerical results will be given in Section V-D.

C. The Optimal Antenna Downtilt

Considering the results of $p^{\text{cov}}\left(\lambda_B, \gamma\right)$ shown in Eq.(12) , θ_{tilt} is the only variable for certain values of λ_B and γ. A large antenna downtilt reduces inter-cell interference power, while at the same time decreases signal powers for cell edge UEs. On the other hand, a small antenna downtilt leads to the opposite case. Therefore, different antenna downtilts achieve different tradeoffs between the signal power and the interference power, and hence there exists an optimal antenna downtilt to achieve the maximal coverage probability for each BS density. However, the math derivation is not tractable when using the antenna model in Eq.(6). In the following, we will use Gaussian approximation to approximate the antenna downtilt gain $G(\varphi, \theta, \theta_{tilt})$ to obtain tractable results first. Then we will present the optimal antenna downtilt respecting to the BS density, which is summarized as Theorem 6.

Using the parameters in [10] and the curve fitting function in MATLAB, the antenna downtilt gain $G(\varphi, \theta, \theta_{tilt})$ can be approximated by a Gaussian function as

$$G(\varphi, \theta, \theta_{tilt}) \approx a \exp\left[-\frac{(\theta - \theta_{tilt})^2}{b}\right] + c \tag{26}$$

where $a = 6.208$, $b = 116.64$ and $c = 0.4142$.

Thanks to Eq.(26), it is now possible to calculate the derivative of the 3-fold integral computation in Eq.(12), which improves the tractability of our results. In order to get the optimal antenna downtilt to maximize the coverage probability, we take the derivative of the coverage probability and find the optimal point for each BS density.

Theorem 6. *For a certain BS density λ, there exists an optimal antenna downtilt that can maximize the coverage probability, and the optimal antenna downtilt satisfies the following equation:*

$$dP_c^L(\theta_{tilt}) + dP_c^{NL}(\theta_{tilt}) + dP_c^{Noise}(\theta_{tilt}) = 0 \tag{27}$$

where

$$
\begin{aligned}
dP_c^L(\theta_{tilt}) = \int_0^{d_1} \int_r^\infty & \left(\sqrt{(L^2 + r^2)}^{\alpha_L} \right) \left[(\theta_v - \theta_r) \exp\left[-\frac{(\theta_v - \theta_r)(\theta_v + \theta_r - 2\theta_{tilt})}{b} \right] \right. \\
& + a \left(\exp\left[-\frac{(\theta_v - \theta_{tilt})^2}{b} \right] (\theta_v - \theta_{tilt}) - \exp\left[-\frac{(\theta_r - \theta_{tilt})^2}{b} \right] (\theta_r - \theta_{tilt}) \right) \Big] \\
& \times f_{R,1}^{\mathrm{L}}(r) \, dv dr
\end{aligned}
\tag{28}
$$

and

$$
\begin{aligned}
dP_c^{NL}(\theta_{tilt}) = \int_0^{d_1} \int_r^\infty & \left(\sqrt{(L^2 + r^2)}^{\alpha_{NL}} \right) \left[(\theta_v - \theta_r) \exp\left[-\frac{(\theta_v - \theta_r)(\theta_v + \theta_r - 2\theta_{tilt})}{b} \right] \right. \\
& + a \left(\exp\left[-\frac{(\theta_v - \theta_{tilt})^2}{b} \right] (\theta_v - \theta_{tilt}) - \exp\left[-\frac{(\theta_r - \theta_{tilt})^2}{b} \right] (\theta_r - \theta_{tilt}) \right) \Big] \\
& \times f_{R,1}^{\mathrm{NL}}(r) \, dv dr \\
& + \int_{d_1}^\infty \int_r^\infty \left(\sqrt{(L^2 + r^2)}^{\alpha_{NL}} \right) \left[(\theta_v - \theta_r) \exp\left[-\frac{(\theta_v - \theta_r)(\theta_v + \theta_r - 2\theta_{tilt})}{b} \right] \right. \\
& + a \left(\exp\left[-\frac{(\theta_v - \theta_{tilt})^2}{b} \right] (\theta_v - \theta_{tilt}) - \exp\left[-\frac{(\theta_r - \theta_{tilt})^2}{b} \right] (\theta_r - \theta_{tilt}) \right) \Big] \\
& \times f_{R,2}^{\mathrm{NL}}(r) \, dv dr
\end{aligned}
\tag{29}
$$

and

$$dP_c^{Noise}(\theta_{tilt}) = \int_0^{d_1} \left(\sqrt{(L^2 + r^2)}^{\alpha_L} \right) \frac{aN_0 \exp\left[-\frac{(\theta_r - \theta_{tilt})^2}{b} \right] \frac{2(\theta_r - \theta_{tilt})}{b}}{P_B A_L \left(a\exp\left[-\frac{(\theta_r - \theta_{tilt})^2}{b} \right] + c \right)^2} f_{R,1}^L (r)\, dr$$

$$+ \int_0^{d_1} \left(\sqrt{(L^2 + r^2)}^{\alpha_{NL}} \right) \frac{aN_0 \exp\left[-\frac{(\theta_r - \theta_{tilt})^2}{b} \right] \frac{2(\theta_r - \theta_{tilt})}{b}}{P_B A_{NL} \left(a\exp\left[-\frac{(\theta_r - \theta_{tilt})^2}{b} \right] + c \right)^2} f_{R,1}^{NL} (r)\, dr$$

$$+ \int_{d_1}^{\infty} \left(\sqrt{(L^2 + r^2)}^{\alpha_{NL}} \right) \frac{aN_0 \exp\left[-\frac{(\theta_r - \theta_{tilt})^2}{b} \right] \frac{2(\theta_r - \theta_{tilt})}{b}}{P_B A_{NL} \left(a\exp\left[-\frac{(\theta_r - \theta_{tilt})^2}{b} \right] + c \right)^2} f_{R,2}^{NL} (r)\, dr \quad (30)$$

where $f_{R,1}^L (r)$, $f_{R,1}^{NL} (r)$ and $f_{R,2}^{NL} (r)$ can be found in Theorem 1 and $a = 6.208$, $b = 116.64$, $c = 0.4142$.

Proof: See Appendix B. ∎

From Theorem 6, we can draw the following insights:

- There are three components in Eq.(27) which lead to the optimal antenna downtilt, including the LoS part shown as Eq.(28), the NLoS part shown as Eq.(29) and the noise part shown as Eq.(30), respectively.

- When the networks are sparse, the signal is mostly NLoS and the noise is the dominant factor. Therefore, the NLoS and noise parts of Eq.(27) are the major ones that determine the optimal downtilt.

- As the BS density increases, most signals and a part of interference links transit from NLoS to LoS, and hence, all components in Eq.(27) should be taken into account.

- When the BS density is large enough, almost all signals and the major interference links are LoS, and the noise is very small compared to the signal or interference. Therefore, the LoS part of Eq.(27) is the major component that determines the optimal downtilt.

Theorem 6 is numerically solvable and we can use the 'fslove' function in MATLAB to obtain the results.

D. The Area Spectral Efficiency

As mentioned in Eq.(11), we investigate the area spectral efficiency (ASE) performance in bps/Hz/km^2, which is defined as

$$A^{\text{ASE}}\left(\lambda_B, \gamma_0\right) = \lambda_B \int_{\gamma_0}^{+\infty} \log_2\left(1 + \gamma\right) f_\Gamma\left(\lambda_B, \gamma\right) d\gamma, \tag{31}$$

where γ_0 is the minimum working SINR for the considered UDNs, and $f_\Gamma\left(\lambda, \gamma\right)$ is the probability density function (PDF) of the SINR observed at the typical UE at a particular value of λ_B. Based on the definition of $p^{\text{cov}}\left(\lambda_B, \gamma\right)$ in Eq.(8), which is the complementary cumulative distribution function (CCDF) of SINR, $f_\Gamma\left(\lambda_B, \gamma\right)$ can be computed by

$$f_\Gamma\left(\lambda_B, \gamma\right) = \frac{\partial\left(1 - p^{\text{cov}}\left(\lambda_B, \gamma\right)\right)}{\partial\gamma}. \tag{32}$$

where $p^{\text{cov}}\left(\lambda_B, \gamma\right)$ can be obtained from Theorem 1.

V. SIMULATION AND DISCUSSION

In this section, numerical results are provided to validate the accuracy of our analysis and to verify the intuitive performance trends discussed in Section IV. The analytical results are compared against Monte Carlo simulation results in the coverage probability. According to [10], we adopt the following parameters for 3GPP Case 1: $d_1 = 300m$, $\alpha^L = 2$, $\alpha^{NL} = 3.75$, $A^L = 10^{-10.38}$, $A^{NL} = 10^{-14.54}$, $P_B = 24dBm$, $P_N = -95dBm$ (including a noise figure of 9 dB at the receivers).

A. Validation of Theorem 1 on the Coverage Probability

In this subsection, we investigate the coverage probability and validate the analytical results in Theorem 1 by comparing with Monte Carlo simulation results. In Fig.2, we plot the results of the coverage probability for five BS densities with $\gamma = 0dB$. Regarding the non-zero value of L, as explained in Section I, the BS antenna and the UE antenna heights are set to 10m and 1.5m, respectively [10]. As can be observed from Fig.2, our analytical results given by Theorem 1 match the simulation results very well, and we can draw the following observations:

- For a certain BS density, there only exists one optimal antenna downtilt which can achieve the maximum coverage probability. In essence, a large antenna downtilt reduces
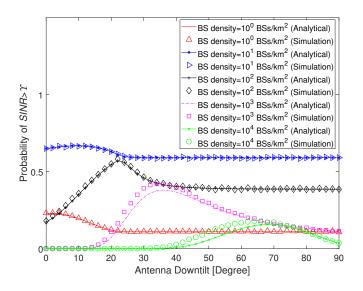
Figure 2. Coverage probability vs. antenna downtilt with $\gamma = 0dB$

inter-cell interference power, while at the same time decreases signal powers for cell edge UEs. On the other hand, a small antenna downtilt leads to the opposite case. Therefore, a different antenna downtilt achieves a different balance between the signal power and the interference power.

- Antenna downtilt has a significant impact on the coverage probability and the optimal antenna downtilt increases as the BS density increases from nearly zero degree to 90 degrees.

B. *Validation of Theorem 6 on the Optimal Antenna Downtilt*

In this subsection, we validate the analytical results in Theorem 6 by comparing with Monte Carlo simulation results.
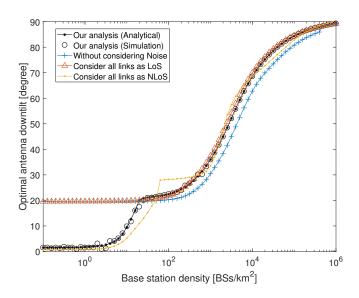
Figure 3. Optimal antenna downtilt vs. base station density with $\gamma = 0dB$

In Fig.3, we show the optimal downtilt with the BS density increases with $\gamma = 0dB$. As we can observed from Fig.3, our analytical results given by Theorem 6 match the simulation results very well, which validates the accuracy of our analysis. Moreover, we can draw the following observations:

- The optimal antenna downtilt increases as the BS density increases, and when the BS density is around 10^6 BSs/km^2, the optimal antenna downtilt approaches 90 degree.

- From Fig.3, the curve which considers all links as NLoS matches results in Theorem 6 when the BSs are sparse. This is due to the fact that the signal is mostly NLoS and the noise is the dominant factor. Therefore, the NLoS and noise parts in Eq.(27) are the major ones that determine the optimal downtilt.

- From around $10^{0.3}BSs/km^2$ to around $10^{1.1}BSs/km^2$, most signals and interference are NLoS when the BS density is $10^{0.3}BSs/km^2$ and then some signals transit from NLoS to LoS and hence increasing the signal power. The main benefit of the antenna downtilt is to decrease the dominant interference as the LoS signal is strong enough. During this range, both the LoS/NLoS and noise parts in Eq.(27) should be considered.

- When the BS density is around $10^{1.1}BSs/km^2$, the increasing speed of the optimal antenna downtilt is slowing down because most signals and the dominant interference have transited from NLoS to LoS, and thus the main purpose of the antenna downtilt shifts from strengthening the signal power to reducing the interference power.

- When the BS density is larger than around $10^{1.1} BSs/km^2$, almost all signals are LoS and more and more interference transit from NLoS to LoS as the BS density increases. The noise is very small compared to the signal or interference so that the LoS part in Theorem 6 is the major one to determine the optimal antenna downtilt. As we see from Fig.3, when we consider all links as LoS, the optimal antenna downtilt results are almost same with the results that achieved based on the model we proposed.

C. The Gain of Signal Strength Using Antenna Downtilt

Fig.4 shows the received signal gain of the typical UE with the BS density which has been analyzed in Eq.(20). From Fig.4, we can see that:
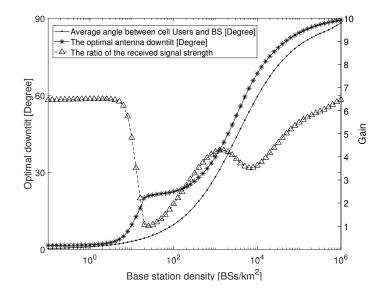

Figure 4. Signal gain vs. base station density

- When the network is relatively sparse, e.g., from around $0\ BSs/km^2$ to around $10^{0.3} BSs/km^2$, all links are NLoS. In this case, through adjusting the antenna downtilt, UE can achieve the maximum antenna downtilt gain on the received signal, which is around 6.5.
- From $10^{0.3}$~$10^{1.1} BSs/km^2$, the received signal gain brought by the optimal antenna downtilt decreases because most signal and the dominant interference path from NLoS to LoS, the main benefit of the antenna downtilt is to decrease the dominant interference.
- In the third stage, e.g., from around $10^{1.1} BSs/km^2$ to around $10^3 BSs/km^2$, the received signal gain brought by the optimal antenna downtilt increases slowly, which means that

the increases of the signal outweighs the decrease of the interference when adopting the optimal antenna downtilt.

- Then from around $10^3 BSs/km^2$ to around $10^{3.7} BSs/km^2$, the received signal gain decreases slightly because most interference transit from NLoS to LoS so that the increase of the aggregation interference outweighs the decrease of the signal when adopting the optimal antenna downtilt.

- In the fifth stage, e.g., from around $10^{3.7} BSs/km^2$ to around $10^6 BSs/km^2$, all links are LoS. In this case, the received signal gain increases as the BS density increases to obtain the best coverage probability.

D. The Reduction of Interference Using Antenna Downtilt

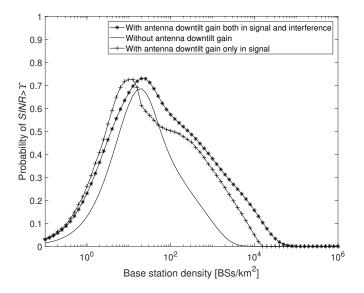Fig.5 shows the coverage probability without antenna downtilt gain on interference. From

Figure 5. The impact of the optimal antenna downtilt on the interference

Fig.5, we can see that:

- From $0 \sim 10^{1.1} BSs/km^2$, the gain on the received signal brought by the optimal antenna downtilt is smaller than the gain on the interference, therefore the main purpose of antenna downtilt is to decrease the interference.

- After $10^{1.1} BSs/km^2$, the gain on the received signal brought by the optimal antenna downtilt is larger than the gain on the interference due to interference reduction. The

optimal antenna downtilt brings down the interference so that improves the coverage probability.

E. Network Performance with the Optimal Network-Wide Antenna Downtilt

In this subsection, we investigate the coverage probability and the ASE with the optimal antenna downtilt compared with the results in [2].
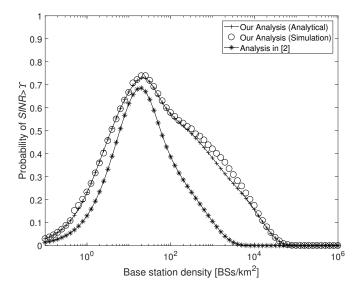

Figure 6. Coverage probability vs. base station density with optimal antenna downtilt

1) The coverage probability with the Optimal Network-Wide Antenna Downtilt: Fig.6 shows the coverage probability with the optimal antenna downtilt and without any downtilt. As we can observe from Fig.6:

- The antenna downtilt does not change the trend of the coverage probability, i.e., it first increases and then decreases to zero as BS density increases.

- The coverage probability performance with the optimal antenna downtilt is always better than that without antenna downtilt. The coverage probability reaches zero when the BS density is $3 \times 10^4 BSs/km^2$, while it is around $3 \times 10^3 BSs/km^2$ in the previous work [2].

- Applying the optimal antenna downtilt decreases the rate of decline of the coverage probability when the BS density is larger than $100 BSs/km^2$.

2) The ASE with the Optimal Network-Wide Antenna Downtilt: In the following, we investigate the ASE performance with the optimal antenna downtilt.
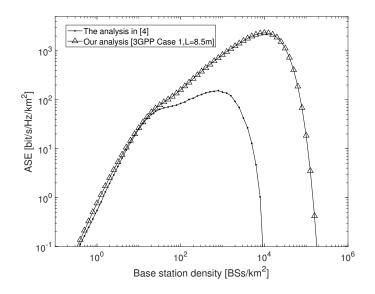
Figure 7. $A^{ASE}(\lambda, \gamma_0)$ vs. base station density with optimal antenna downtilt

Fig.7 shows the ASE with and without optimal antenna downtilt. From Fig.7, we can draw the following observations:

- After using the optimal antenna downtilt, the ASE increases as BS density increases until 2×10^4 BSs/km^2, then it decreases to zero when BS density is around 2×10^5 BSs/km^2.

- The optimal antenna downtilt improves the ASE significantly and delay the ASE crash by nearly one order of magnitude in terms of the base station density.

F. Network Performance with the Empirical BS-Specific Antenna Downtilt

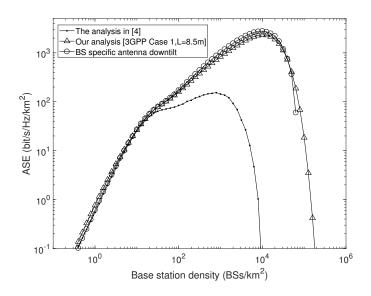In this subsection, we investigate the ASE performance with BS-specific antenna downtilts.

Figure 8. $A^{ASE}(\lambda, \gamma_0)$ vs. base station density with optimal antenna downtilt and BS specific empirical downtilt

In particular, for a certain BS density, adjusting the antenna downtilt of each base station according to each cell's coverage area may further improve the performance compared with using an uniform downtilt for all BSs. For example, for each downlink cell, the BS can adjust its antenna downtilt based on the distribution of UEs in this particular cell to maximize the serving signal, instead of using an uniform downtilt for all cells. In Fig.8, we investigate the performance of $A^{ASE}(\lambda, \gamma_0)$ under the same assumptions except the choice of antenna downtilt, which uses the BS specific empiric downtilt. Particularly, each BS adopt an empirical downtilt as [2], which is formulated as

$$\theta_{tilt} = arctam\left(\frac{L}{r}\right) + zB_V \qquad (33)$$

where r is the equivalent radius of each cell, z is set to 0.7 as an empirical value, B_V is the vertical half-wave dipole antenna, for 4-element, $B_V = 19.5°$. Fig. 9 illustrates such empirical antenna downtilt. However, the results showed in Fig.8 give a sense that the trend of ASE is not changed. From Fig.8, our key conclusions are drawn as follows:

- Applying the BS specific empirical antenna downtilt will not change the trend of ASE as the BS density increases, and the ASE will decrease towards zero when the BS density is around 2×10^5 BSs/km^2.

- Regarding antenna downtilt, it is not necessary to optimize it on a per-BS basis as the performance of ASE is not improved much compared with a network-wide optimal
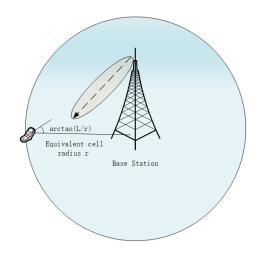
Figure 9. An illustrative figure for the empirical equation

antenna downtilt.

VI. CONCLUSION

In this paper, we have investigated the impact of the practical antenna pattern and downtilt on the performance of DL cellular networks. We found that there is an optimal antenna downtilt to achieve the maximal coverage probability for each BS density. Analytical results have been obtained for the optimal antenna downtilt, the coverage probability and the ASE performance. Our results have shown that there are three parts determining the optimal antenna downtilt, and the optimal antenna downtilt increases as the BS density grows. Compared with previous works in [7], we found that using the optimal antenna downtilt can improve the ASE performance significantly. Specifically, it can delay the ASE crash by nearly one order of magnitude in terms of the BS density. As our future work, we will consider the optimal antenna height in the cellular networks.

APPENDIX A: PROOF OF THEOREM 1

Proof: Based on the UAS and the path loss model, the distance of the signal can be divided into two parts, namely $[0, d_1]$ and $[d_1, \infty]$. In the first path, there are both LoS and NLoS signal while in the second path, there is only NLoS signal. For the LoS signal in the

first path,

$$
\Pr\left[\left.\frac{\mathsf{S}^{\mathsf{L}}}{I_L + I_N + N_0} > \gamma \right| r\right]
$$

$$
= \Pr\left[\left.\frac{P_B g G(\varphi, \theta_r, \theta_{tilt}) A^L \sqrt{r^2 + L^2}^{-\alpha^L}}{I_L + I_N + N_0} > \gamma \right| r\right]
$$

$$
= \Pr\left[\left. g > \frac{\gamma\left(I_L + I_N + N_0\right)}{P_B G(\varphi, \theta_r, \theta_{tilt}) A^L \sqrt{r^2 + L^2}^{-\alpha^L}} \right| r\right]
$$

$$
= \mathbb{E}_{\mathrm{I}}\left[\left. \exp\left(-\frac{\gamma\left(\mathrm{I_L + I_N + N_0}\right)}{\mathrm{P_B G(\varphi, \theta_r, \theta_{tilt}) A^L \sqrt{r^2 + L^2}^{-\alpha^L}}}\right) \right| \mathrm{r}\right]
$$

$$
= \exp\left(-\frac{\gamma \mathrm{N_0}}{\mathrm{P_B G(\varphi, \theta_r, \theta_{tilt}) A^L \sqrt{r^2 + L^2}^{-\alpha^L}}}\right) \mathscr{L}_{I_{\mathrm{agg}}}\left(s\right), \qquad (34)
$$

where $s = \frac{\gamma}{\mathrm{P_B G(\varphi, \theta_r, \theta_{tilt}) A^L \sqrt{r^2 + L^2}^{-\alpha^L}}}$,

$$
\mathscr{L}_{I_{\mathrm{agg}}}\left(s\right) = \mathbb{E}_{[\mathrm{I}_r]}\left\{\left.\exp\left(-s\mathrm{I}_r\right)\right| 0 < r < d_1\right\}
$$

$$
= \mathbb{E}_{[\phi, \{g\}, \{\zeta(u)G(\varphi, \theta_u, \theta_{tilt})\}]}\left\{\left.\exp\left(-sP_B g \zeta\left(u\right) G(\varphi, \theta_u, \theta_{tilt})\right)\right| 0 < r < d_1\right\}
$$

$$
= \exp\left(-2\pi\lambda_B \int_r^\infty \left(1 - \mathbb{E}_{[\{g\}]}\left\{\exp\left(-sP_B g \zeta\left(u\right) G(\varphi, \theta_u, \theta_{tilt})\right)\right\}\right) u du \,\middle|\, 0 < r < d_1\right)
$$

$$
= \exp\left(-2\pi\lambda_B \int_r^{d_1} (1 - \frac{\sqrt{u^2 + L^2}}{d_1})\frac{u}{1 + \left(sP_B A^L G(\varphi, \theta_u, \theta_{tilt})\right)^{-1}\sqrt{u^2 + L^2}^{\alpha_L}} du\right)
$$

$$
\times \exp\left(-2\pi\lambda_B \int_{r_1}^{d_1} (\frac{\sqrt{u^2 + L^2}}{d_1})\frac{u}{1 + \left(sP_B A^{NL} G(\varphi, \theta_u, \theta_{tilt})\right)^{-1}\sqrt{u^2 + L^2}^{\alpha_{NL}}} du\right)
$$

$$
\times \exp\left(-2\pi\lambda_B \int_{d_1}^\infty \frac{u}{1 + \left(sP_B A^{NL} G(\varphi, \theta_u, \theta_{tilt})\right)^{-1}\sqrt{u^2 + L^2}^{\alpha_{NL}}} du\right) \qquad (35)
$$

For the NLoS signal in the first path, in the range of $0 < r \leq y_1$, y_1 means $r_2 = d_1$.

$$\Pr\left[\frac{S^{NL}}{I_L + I_N + N_0} > \gamma \,\middle|\, r\right]$$

$$= \Pr\left[\frac{P_B g G(\varphi, \theta_r, \theta_{tilt}) A^{NL} \sqrt{r^2 + L^2}^{-\alpha^{NL}}}{I_L + I_N + N_0} > \gamma \,\middle|\, r\right]$$

$$= \Pr\left[g > \frac{\gamma(I_L + I_N + N_0)}{P_B G(\varphi, \theta_r, \theta_{tilt}) A^{NL} \sqrt{r^2 + L^2}^{-\alpha^{NL}}} \,\middle|\, r\right]$$

$$= \mathbb{E}_I\left[\exp\left(-\frac{\gamma(I_L + I_N + N_0)}{P_B G(\varphi, \theta_r, \theta_{tilt}) A^{NL} \sqrt{r^2 + L^2}^{-\alpha^{NL}}}\right) \,\middle|\, r\right]$$

$$= \exp\left(-\frac{\gamma N_0}{P_B G(\varphi, \theta_r, \theta_{tilt}) A^{NL} \sqrt{r^2 + L^2}^{-\alpha^{NL}}}\right) \mathscr{L}_{I_{agg}}(s), \quad (36)$$

where $s = \frac{T}{P_B G(\varphi, \theta_r, \theta_{tilt}) A^{NL} \sqrt{r^2 + L^2}^{-\alpha^{NL}}}$,

$$\mathscr{L}_{I_{agg}}(s) = \mathbb{E}_{[I_r]}\left\{\exp\left(-sI_r\right) \middle| 0 < r < y_1\right\}$$

$$= \mathbb{E}_{[\phi, \{g\}, \{\zeta(u)G(\varphi, \theta_u, \theta_{tilt})\}]}\left\{\exp\left(-sP_B g \zeta(u) G(\varphi, \theta_u, \theta_{tilt})\right) \middle| 0 < r < y_1\right\}$$

$$= \exp\left(-2\pi\lambda_B \int_r^\infty \left(1 - \mathbb{E}_{[\{g\}]}\left\{\exp\left(-sP_B g \zeta(u) G(\varphi, \theta_u, \theta_{tilt})\right)\right\}\right) u\,du \,\middle|\, 0 < r < y_1\right)$$

$$= \exp\left(-2\pi\lambda_B \int_{r_2}^{d_1} (1 - \frac{\sqrt{u^2 + L^2}}{d_1}) \frac{u}{1 + (sP_B A^L G(\varphi, \theta_u, \theta_{tilt}))^{-1} \sqrt{u^2 + L^2}^{\alpha_L}} du\right)$$

$$\times \exp\left(-2\pi\lambda_B \int_r^{d_1} (\frac{\sqrt{u^2 + L^2}}{d_1}) \frac{u}{1 + (sP_B A^{NL} G(\varphi, \theta_u, \theta_{tilt}))^{-1} \sqrt{u^2 + L^2}^{\alpha_{NL}}} du\right)$$

$$\times \exp\left(-2\pi\lambda_B \int_{d_1}^\infty \frac{u}{1 + (sP_B A^{NL} G(\varphi, \theta_u, \theta_{tilt}))^{-1} \sqrt{u^2 + L^2}^{\alpha_{NL}}} du\right) \quad (37)$$

and when in the range of $y_1 < r \le d_1$,

$$\Pr\left[\frac{S^{NL}}{I_N + N_0} > \gamma \middle| r\right]$$

$$= \Pr\left[\frac{P_B g G(\varphi, \theta_r, \theta_{tilt}) A^{NL} \sqrt{r^2 + L^2}^{-\alpha^{NL}}}{I_N + N_0} > \gamma \middle| r\right]$$

$$= \Pr\left[h > \frac{\gamma(I_N + N_0)}{P_B G(\varphi, \theta_r, \theta_{tilt}) A^{NL} \sqrt{r^2 + L^2}^{-\alpha^{NL}}} \middle| r\right]$$

$$= \mathbb{E}_I\left[\exp\left(-\frac{\gamma(I_N + N_0)}{P_B G(\varphi, \theta_r, \theta_{tilt}) A^{NL} \sqrt{r^2 + L^2}^{-\alpha^{NL}}}\right) \middle| r\right]$$

$$= \exp\left(-\frac{\gamma N_0}{P_B G(\varphi, \theta_r, \theta_{tilt}) A^{NL} \sqrt{r^2 + L^2}^{-\alpha^{NL}}}\right) \mathscr{L}_{I_{agg}}(s), \qquad (38)$$

where $s = \frac{\gamma}{P_B G(\varphi, \theta_r, \theta_{tilt}) A^{NL} \sqrt{r^2 + L^2}^{-\alpha^{NL}}}$,

$$\mathscr{L}_{I_{agg}}(s) = \mathbb{E}_{[I_r]}\left\{\exp(-sI_r) \middle| y_1 < r \le d_1\right\}$$

$$= \mathbb{E}_{[\phi, \{g\}, \{\zeta(u)G(\varphi, \theta_u, \theta_{tilt})\}]}\left\{\exp(-sP_B g\zeta(u)G(\varphi, \theta_u, \theta_{tilt})) \middle| y_1 < r \le d_1\right\}$$

$$= \exp\left(-2\pi\lambda_B \int_r^\infty \left(1 - \mathbb{E}_{[\{g\}]}\left\{\exp(-sP_B g\zeta(u)G(\varphi, \theta_u, \theta_{tilt}))\right\}\right) u\,du \middle| y_1 < r \le d_1\right)$$

$$= \exp\left(-2\pi\lambda_B \int_r^{d_1} (\frac{\sqrt{u^2 + L^2}}{d_1}) \frac{u}{1 + (sP_B A^{NL}G(\varphi, \theta_u, \theta_{tilt}))^{-1}\sqrt{u^2 + L^2}^{\alpha_{NL}}}\,du\right)$$

$$\times \exp\left(-2\pi\lambda_B \int_{d_1}^\infty \frac{u}{1 + (sP_B A^{NL}G(\varphi, \theta_u, \theta_{tilt}))^{-1}\sqrt{u^2 + L^2}^{\alpha_{NL}}}\,du\right) \qquad (39)$$

For the NLoS signal in the second path, in the range of $r > d_1$,

$$\Pr\left[\frac{S^{NL}}{I_N + N_0} > \gamma \middle| r\right]$$

$$= \Pr\left[\frac{P_B g G(\varphi, \theta_r, \theta_{tilt}) A^{NL} \sqrt{r^2 + L^2}^{-\alpha^{NL}}}{I_N + N_0} > \gamma \middle| r\right]$$

$$= \Pr\left[g > \frac{\gamma(I_N + N_0)}{P_B G(\varphi, \theta_r, \theta_{tilt}) A^{NL} \sqrt{r^2 + L^2}^{-\alpha^{NL}}} \middle| r\right]$$

$$= \mathbb{E}_I\left[\exp\left(-\frac{\gamma(I_N + N_0)}{P G(\varphi, \theta_r, \theta_{tilt}) A^{NL} \sqrt{r^2 + L^2}^{-\alpha^{NL}}}\right) \middle| r\right]$$

$$= \exp\left(-\frac{\gamma N_0}{P_B G(\varphi, \theta_r, \theta_{tilt}) A^{NL} \sqrt{r^2 + L^2}^{-\alpha^{NL}}}\right) \mathscr{L}_{I_{agg}}(s), \qquad (40)$$

where $s = \frac{\gamma}{P_B G(\varphi, \theta_r, \theta_{tilt}) A^{NL} \sqrt{r^2 + L^2}^{-\alpha^{NL}}}$,

$$\mathscr{L}_{I_{agg}}(s) = \mathbb{E}_{[I_r]} \left\{ \exp\left(-sI_r\right) | r > d_1 \right\}$$

$$= \mathbb{E}_{[\phi, \{g\}, \{\zeta(u) G(\varphi, \theta_u, \theta_{tilt})\}]} \left\{ \exp\left(-sP_B g \zeta(u) G(\varphi, \theta_u, \theta_{tilt})\right) | r > d_1 \right\}$$

$$= \exp\left(-2\pi\lambda_B \int_r^\infty \left(1 - \mathbb{E}_{[\{g\}]} \left\{ \exp\left(-sP_B g \zeta(u) G(\varphi, \theta_u, \theta_{tilt})\right)\right\}\right) u du \bigg| r > d_1 \right)$$

$$= \exp\left(-2\pi\lambda_B \int_{d_1}^\infty \frac{u}{1 + \left(sP_B A^{NL} G(\varphi, \theta_u, \theta_{tilt})\right)^{-1} \sqrt{u^2 + L^2}^{\alpha_{NL}}} du \right) \quad (41)$$

which concludes our proof.   ∎

APPENDIX B: PROOF OF THEOREM 6

Proof: In Theorem 1

$$p^{cov}(\lambda_B, \gamma) = \int_0^{d_1} \Pr\left[\frac{S^L}{I_L + I_N + N_0} > \gamma \bigg| r \right] f_{R,1}^L(r) dr$$

$$+ \int_0^{d_1} \Pr\left[\frac{S^{NL}}{I_L + I_N + N_0} > \gamma \bigg| r \right] f_{R,1}^{NL}(r) dr$$

$$+ \int_{d_1}^\infty \Pr\left[\frac{S^{NL}}{I_L + I_N + N_0} > \gamma \bigg| r \right] f_{R,2}^{NL}(r) dr. \quad (42)$$

To get the derivative of $p^{cov}(\lambda_B, \gamma)$ respect to θ_{tilt}, we let λ_B, γ be constants. Except the signal, the other factors which lead to the optimal antenna downtilt can be divided into the noise part Ω_{noise}, the LoS interference part $\Omega_{I_{LoS}}$ and the NLoS interference parts $\Omega_{I_{NLoS_1}}(u < d_1)$ and $\Omega_{I_{NLoS_2}}(u > d_1)$, where u is the distance from interference BS to the typical UE. Then we let the derivative of Eq.(42) be zero, therefore the three parts in Eq.(42) are all zero. Take the first part of Eq.(42) as an example, from Eq.(18)

$$p_1^{cov}(\lambda_B, \gamma) = \int_0^{d_1} \exp\left\{ \Omega_{noise} + \Omega_{I_{LoS}} + \Omega_{I_{NLoS_1}} + \Omega_{I_{NLoS_2}} \right\} f_{R,1}^L(r) dr \quad (43)$$

and

$$\int_0^{d_1} \left\{ \Omega_{noise} + \Omega_{I_{LoS}} + \Omega_{I_{NLoS_1}} + \Omega_{I_{NLoS_2}} \right\}'_{\theta_{tilt}} f_{R,1}^L(r) dr = 0 \quad (44)$$

where

$$\Omega_{noise} + \Omega_{I_{LoS}} + \Omega_{I_{NLoS_1}} + \Omega_{I_{NLoS_2}}$$

$$= -2\pi\lambda \int_r^{d_1} (1 - \frac{\sqrt{u^2 + L^2}}{d_1}) \frac{u}{1 + \frac{G(\varphi,\theta_r,\theta_{tilt})\sqrt{u^2+L^2}^{\alpha_L}}{\gamma G(\varphi,\theta_u,\theta_{tilt})\sqrt{r^2+L^2}^{\alpha_L}}} du$$

$$-2\pi\lambda \int_{r_1}^{d_1} (\frac{\sqrt{u^2 + L^2}}{d_1}) \frac{u}{1 + \frac{G(\varphi,\theta_r,\theta_{tilt})A^L\sqrt{u^2+L^2}^{\alpha_{NL}}}{\gamma A^{NL}G(\varphi,\theta_u,\theta_{tilt})\sqrt{r^2+L^2}^{\alpha_L}}} du$$

$$-2\pi\lambda \int_{d_1}^{\infty} \frac{u}{1 + \frac{G(\varphi,\theta_r,\theta_{tilt})A^L\sqrt{u^2+L^2}^{\alpha_{NL}}}{G(\varphi,\theta_u,\theta_{tilt})A^{NL}\gamma\sqrt{r^2+L^2}^{\alpha_L}}} du$$

$$-\frac{\gamma N_0}{P_B G(\varphi,\theta_r,\theta_{tilt})A^L\sqrt{r^2 + L^2}^{-\alpha_L}} \tag{45}$$

using the Eq.(26), we have

$$G(\varphi,\theta_r,\theta_{tilt})' = \frac{2a}{b}(\theta_r - \theta_{tilt})\exp\left[-\frac{(\theta_r - \theta_{tilt})^2}{b}\right] \tag{46}$$

and

$$G(\varphi,\theta_u,\theta_{tilt})' = \frac{2a}{b}(\theta_u - \theta_{tilt})\exp\left[-\frac{(\theta_u - \theta_{tilt})^2}{b}\right] \tag{47}$$

where $\theta_r = \arctan\left(\frac{L}{r}\right)$ and $\theta_u = \arctan\left(\frac{L}{u}\right)$. Plugging Eq.(46) and Eq.(47) into Eq.(44), and considering all the three parts, we have the Theorem 6, which concludes our proof. ∎

REFERENCES

[1] ArrayComm & William Webb. Ofcom, 2007.

[2] David López-Pérez, Ming Ding, Holger Claussen, and Amir H Jafari. Towards 1 Gbps/UE in cellular systems: Understanding ultra-dense small cell deployments. *IEEE Communications Surveys & Tutorials*, 17(4):2078–2101, 2015.

[3] X. Ge, S. Tu, G. Mao, C. X. Wang, and T. Han. 5G ultra-dense cellular networks. *IEEE Wireless Communications*, 23(1):72–79, February 2016.

[4] X. Zhang and J. G. Andrews. Downlink cellular network analysis with multi-slope path loss models. *IEEE Transactions on Communications*, 63(5):1881–1894, May 2015.

[5] T. Bai and R. W. Heath. Coverage and rate analysis for millimeter-wave cellular networks. *IEEE Transactions on Wireless Communications*, 14(2):1100–1114, Feb 2015.

[6] M. Ding and D. López-Pérez. Performance impact of base station antenna heights in dense cellular networks. *IEEE Transactions on Wireless Communications*, 16(12):8147–8161, Dec 2017.

[7] M. Ding, P. Wang, D. López-Pérez, G. Mao, and Z. Lin. Performance impact of LoS and NLoS transmissions in dense cellular networks. *IEEE Transactions on Wireless Communications*, 15(3):2365–2380, Mar. 2016.

[8] I. Atzeni, J. Arnau, and M. Kountouris. Performance analysis of ultra-dense networks with elevated base stations. In *2017 15th International Symposium on Modeling and Optimization in Mobile, Ad Hoc, and Wireless Networks (WiOpt)*, pages 1–6, May 2017.

[9] A. D. Gandhi. Significant gains in coverage and downlink capacity from optimal antenna downtilt for closely-spaced cells in wireless networks. In *2014 23rd Wireless and Optical Communication Conference (WOCC)*, pages 1–6, May 2014.

[10] 3GPP. TR 36.814: Further advancements for E-UTRA physical layer aspects (Release 9), Mar. 2010.

[11] H. C. Nguyen, I. Rodriguez, T. B. Sorensen, J. Elling, M. B. Gentsch, M. Sorensen, and P. Mogensen. Validation of tilt gain under realistic path loss model and network scenario. In *2013 IEEE 78th Vehicular Technology Conference (VTC Fall)*, pages 1–5, Sept 2013.

[12] J. Fan, G. Y. Li, and X. Zhu. Vertical beamforming with downtilt optimization in downlink cellular networks. In *2015 IEEE Global Communications Conference (GLOBECOM)*, pages 1–5, Dec 2015.

[13] J. G. Andrews, F. Baccelli, and R. K. Ganti. A tractable approach to coverage and rate in cellular networks. *IEEE Transactions on Communications*, 59(11):3122–3134, November 2011.

[14] T. D. Novlan, H. S. Dhillon, and J. G. Andrews. Analytical modeling of uplink cellular networks. *IEEE Transactions on Wireless Communications*, 12(6):2669–2679, June 2013.

[15] M. Ding and D. López-Pérez. Please lower small cell antenna heights in 5g. In *2016 IEEE Global Communications Conference (GLOBECOM)*, pages 1–6, Dec 2016.

[16] M. Danneberg, J. Holfeld, M. Grieger, M. Amro, and G. Fettweis. Field trial evaluation of ue specific antenna downtilt in an lte downlink. In *2012 International ITG Workshop on Smart Antennas (WSA)*, pages 274–280, March 2012.

[17] N. Seifi, M. Coldrey, M. Matthaiou, and M. Viberg. Impact of base station antenna tilt on the performance of network mimo systems. In *2012 IEEE 75th Vehicular Technology Conference (VTC Spring)*, pages 1–5, May 2012.

[18] M. Ding, D. López-Pérez, and G. Mao. A new capacity scaling law in ultra-dense networks. *arXiv:1704.00399 [cs.NI]*, Apr. 2017.

[19] M. Ding, D. López-Pérez, G. Mao, P. Wang, and Z. Lin. Will the area spectral efficiency monotonically grow as small cells go dense? *IEEE GLOBECOM 2015*, pages 1–7, Dec. 2015.

[20] Spatial Channel Model AHG. Subsection 3.5.3, Spatial Channel Model Text Description V6.0, Apr. 2003.

[21] 3GPP. TR 36.828: Further enhancements to LTE Time Division Duplex (TDD) for Downlink-Uplink (DL-UL) interference management and traffic adaptation, Jun. 2012.

[22] Fredrik Gunnarsson, Martin N Johansson, Anders Furuskar, Magnus Lundevall, Arne Simonsson, Claes Tidestav, and Mats Blomgren. Downtilted base station antennas-a simulation model proposal and impact on hspa and lte performance. In *Vehicular Technology Conference, 2008. VTC 2008-Fall. IEEE 68th*, pages 1–5. IEEE, 2008.